PHYSICAL REVIEW A VOLUME 59, NUMBER 5 MAY 1999

Semiclassical interferences and catastrophes in the ionization of Rydberg atoms by half-cycle pulses

G. Alber[1] and O. Zobay[2]
[1]*Abteilung für Quantenphysik, Universität Ulm, D-89069 Ulm, Germany*
[2]*Optical Sciences Center, University of Arizona, Tucson, Arizona 85721*
(Received 5 June 1998)

A multidimensional semiclassical description of excitation of a Rydberg electron by half-cycle pulses is developed and applied to the study of energy- and angle-resolved ionization spectra. Characteristic phenomena observable in these spectra such as interference oscillations and semiclassical glory and rainbow scattering are discussed and related to the underlying classical dynamics of the Rydberg electron. Modifications to the predictions of the impulse approximation are examined that arise due to finite pulse durations.
[S1050-2947(99)50205-9]

PACS number(s): 32.80.Rm, 03.65.Sq

High-power, nearly unipolar electromagnetic-field pulses are a useful spectroscopic tool, in particular for studying the dynamics of weakly bound Rydberg electrons. Various experimental [1–3] and theoretical [4,5] investigations on the interaction between Rydberg atoms and half-cycle pulses (HCPs) have already been performed. In particular, the theoretical approaches that have been used so far involve either fully quantum-mechanical calculations, purely classical simulations, or simplified one-dimensional model problems. Fully quantum-mechanical treatments are capable of yielding quantitatively exact results, but due to the large spatial extension of highly excited Rydberg states they demand a huge computational effort. Furthermore, they allow only for a restricted qualitative understanding of the system, in general. Purely classical approaches are of interest, as they yield insight into the underlying classical aspects of the motion of the Rydberg electron. But they cannot deal properly with quantum-mechanical interference effects and are therefore also of limited applicability. One-dimensional model problems, finally, are not capable of describing all spatial aspects of the excitation process. Thus the natural question arises whether a proper three-dimensional theoretical description of the excitation process can be developed that is numerically highly accurate even for very large principal quantum numbers, which gives direct insight into the underlying classical aspects of the dynamics of the Rydberg electron and which is capable of dealing with all quantum-mechanical interference phenomena properly.

In this Rapid Communication it is shown that such a theoretical description can be developed on the basis of a multidimensional semiclassical description of the excitation process. This approach is easily applicable to any spatial or temporal pulse form of the exciting HCP, and it is particularly accurate in the region of high principal quantum numbers, which is difficult to access by fully quantum-mechanical calculations. Based on this treatment different oscillatory structures are discussed, which appear in energy- and angle-resolved ionization spectra and which should be accessible to experimental observation in view of the recently developed imaging method [6]. It is shown that these structures are caused by quantum-mechanical interferences between probability amplitudes that can be associated with classical trajectories of the ionized Rydberg electron. In order to demonstrate the numerical accuracy of the multidimensional semiclassical approach a comparison with numerical results is presented in the impulse approximation. Modifications of these oscillatory structures due to finite pulse durations are also discussed.

Let us consider a typical HCP-excitation process. Initially an atom is prepared in a Rydberg state $|n_0 l_0 m_0\rangle$ with a large principal quantum number $n_0 \gg 1$ and a small angular-momentum quantum number $l_0 \ll n_0$. Around $t=0$ a linearly polarized HCP with vector potential $A(\mathbf{x},t)\mathbf{e}_z$ and duration τ interacts with the Rydberg electron. The time evolution of the state $\psi(\mathbf{x},t)$ of the Rydberg electron is determined by the Schrödinger equation

$$i\dot{\psi}(\mathbf{x},t)=\{\tfrac{1}{2}[-i\boldsymbol{\nabla}_{\mathbf{x}}-A(\mathbf{x},t)\mathbf{e}_z]^2-V_C(\mathbf{x})\}\psi(\mathbf{x},t) \qquad (1)$$

with the effective electronic potential $V_C(\mathbf{x})$ (Hartree atomic units with $e=\hbar=m_e=1$ are used). Assuming axial symmetry of $A(\mathbf{x},t)$ around the z axis, the z component of the electronic angular momentum L_z is conserved. As long as $n_0 \gg 1$, the solution of Eq. (1) can be obtained to a good degree of approximation with the help of semiclassical methods. Thereby, one starts from the semiclassical expression for the initial Rydberg state

$$\langle \mathbf{x}_0|n_0 l_0 m_0\rangle = A_{cl}(\mathbf{x}_0)\{e^{i[S_0(r_0,\epsilon_0)-\pi/4]}+\text{c.c.}\}. \qquad (2)$$

The amplitude of this state is given by [7]

$$A_{cl}(\mathbf{x}_0)=\frac{Y_{l_0}^{m_0}(\Theta_0,\phi_0)}{r_0(n_0-\alpha)^{3/2}\sqrt{2\pi p(r_0,\epsilon_0)}} \qquad (3)$$

with the spherical harmonic $Y_{l_0}^{m_0}$, the radial momentum $p(r_0,\epsilon_0)=\sqrt{2(\epsilon_0+1/r_0)}$, and with the initial energy $\epsilon_0=-[2(n_0-\alpha)^2]^{-1}$ (α denotes the quantum defect of the Rydberg electron). The phases of this state are determined by the classical eikonal $S_0(r_0,\epsilon_0)=\int_0^r dr' p(r',\epsilon_0) -(l_0+1/2)\pi+\pi\alpha$. Equation (2) is valid for distances $r_0=|\mathbf{x}_0|$ of the electron from the nucleus that are located outside the core region and well inside the classically allowed

region. Semiclassically one has to associate with this particular initial state a bivalued field of classical momenta $\mathbf{p}^{(\pm)}(\mathbf{x}_0)=\pm\nabla_{\mathbf{x}_0}S_0(r_0,\epsilon_0)$ that defines a Lagrangian manifold. Generalizations to other types of initial states that lead to other Lagrangian manifolds are possible according to the general framework of multidimensional semiclassical approximations [8]. Thus under the influence of the HCP two classical trajectories $\mathbf{x}_\pm(t;\mathbf{x}_0)$ emanate from each point $\mathbf{x}_0$. They are solutions of the classical equations of motion of the Hamilton function $H=[\mathbf{p}-A(\mathbf{x},t)\mathbf{e}_z]^2/2+V_C(\mathbf{x})$ with initial conditions $(\mathbf{x}_0,\mathbf{p}^{(\pm)}(\mathbf{x}_0))$. From Eq. (1) and Maslov's generalization of the Van-Vleck propagator [8] one obtains the probability amplitude of observing the ionized Rydberg electron with final asymptotic momentum $\mathbf{p}^{(f)}$, namely,

$$\langle\mathbf{p}^{(f)}|\psi(t\to\infty)\rangle=\sum_j P_j^{(cl)}e^{i[S_j+W_j(\mathbf{x}_0^{(j)})-\pi\mu_j/2]}. \qquad (4)$$

As this result is understandable in a straightforward way in physical terms the details of its derivation will be presented elsewhere [9].

The ionization amplitude of Eq. (4) is expressed as a sum of contributions of all classical trajectories j of the Rydberg electron with initial positions $\mathbf{x}_0^{(j)}$ that yield the asymptotic momentum $\mathbf{p}^{(f)}=\mathbf{p}_\pm(t\to\infty;\mathbf{x}_0,\mathbf{p}^{(\pm)}(\mathbf{x}_0))$. The contribution of trajectory j to the classical angle- and energy-resolved ionization amplitude is determined by

$$P_j^{(cl)}=\left|\frac{dp_x^{(f)}\wedge dp_y^{(f)}\wedge dp_z^{(f)}}{dx_0\wedge dy_0\wedge dz_0}\right|_j^{-1/2}A_{cl}(\mathbf{x}_0^{(j)}). \qquad (5)$$

The phases associated with these trajectories are determined by the Morse indices μ_j, by the classical actions

$$S_j=-\int_0^\infty dt\mathbf{x}_j(t)\cdot\frac{d\mathbf{p}^{(j)}}{dt}-\mathbf{x}_0^{(j)}\cdot\mathbf{p}_0^{(j)}, \qquad (6)$$

and by the classical actions of the initial state $W_j(\mathbf{x}_0^{(j)})=\pm[S_0(r_0^{(j)},\epsilon_0)-\pi/4]$. For $W_j(\mathbf{x}_0^{(j)})$ one has to choose the plus or the minus sign, depending on whether the initial radial momentum of the classical trajectory j is positive or negative. The Morse index is equal to the number of sign changes of $dp_x^{(f)}\wedge dp_y^{(f)}\wedge dp_z^{(f)}/dx_0\wedge dy_0\wedge dz_0\equiv\mathrm{Det}[\partial(p_x^{(f)},p_y^{(f)},p_z^{(f)})/\partial(x_0,y_0,z_0)]$ along the trajectory times their multiplicities [8]. In terms of the probability amplitude of Eq. (4) the semiclassical angle- and energy-resolved ionization probability is given by

$$\frac{d^3P_{ion}}{d\epsilon\wedge d\Omega}=\sqrt{2\epsilon^{(f)}}|\langle\mathbf{p}^{(f)}|\psi(t\to\infty)\rangle|^2, \qquad (7)$$

with $\epsilon^{(f)}=\mathbf{p}^{(f)2}/2$ and $d\Omega\equiv\sin\Theta_f d\Theta_f\wedge d\phi_f$. Neglecting all quantum-mechanical interferences between the contributing classical trajectories the classical ionization probability $d^3P_{ion}^{(cl)}/[d\epsilon\wedge d\Omega]=\sqrt{2\epsilon^{(f)}}\Sigma_j(P_j^{(cl)})^2$ is obtained. Without angular resolution this expression has already been used successfully for explaining particular aspects of ionization by half-cycle pulses [2,3]. Equations (4) and (7) constitute an improved, multidimensional semiclassical framework within which all aspects of ionization by an HCP can be understood in terms of the underlying classical dynamics of the ionized Rydberg electron. They constitute a main result of this Rapid Communication. It is worth noting that for all aspects that are sensitive to interferences between different probability amplitudes, such as the angular distributions discussed below, the inclusion of the proper phases entering Eq. (4) is crucial. Furthermore, it should be mentioned that there exists a wealth of alternative methods for solving semiclassical initial-value problems, which have been pioneered by Heller and Miller [10]. However, so far these methods have been applied predominantly to problems with explicitly time-independent Hamiltonians.

In order to demonstrate characteristic phenomena in the angle- and energy-resolved ionization spectra and in order to show the accuracy of this semiclassical approach, let us consider first of all the case of an HCP with a duration short in comparison to the classical orbit time of the Rydberg electron. In this case the sudden ionization or impulse approximation [4] may be invoked. Thereby, the influence of the HCP on the Rydberg electron is described as a sudden momentum change of magnitude $\Delta\mathbf{p}=-\int_{-\infty}^{\infty}dt\mathbf{E}(t)=\Delta p\mathbf{e}_z$ at $t=0$ [$\mathbf{E}(t)$ denotes the electric field of the HCP at the position of the atom]. After the sudden excitation the motion of the electron is governed by the Coulomb potential $V_C(\mathbf{x})$ alone, i.e., $A(\mathbf{x},t)\equiv 0$ for $t>0$ in Eq. (1). Thus, immediately after the HCP, the initial momenta of the classical trajectories appearing in Eq. (4) are given by $\mathbf{p}^{(\pm)}(\mathbf{x}_0)+\Delta\mathbf{p}$. The positions $\mathbf{x}_0^{(j)}$ at which the electron is imparted a final energy $\epsilon^{(f)}$ are determined by energy conservation, i.e.,

$$\epsilon_0+\Delta\mathbf{p}^2/2+\mathbf{p}^{(\pm)}(\mathbf{x}_0^{(j)})\cdot\Delta\mathbf{p}=\epsilon^{(f)}. \qquad (8)$$

Furthermore, consistent with this approximation the classical actions S_j of Eq. (4) have to be replaced by $S_j+\Delta\mathbf{p}\cdot\mathbf{x}_0^{(j)}$.

As a general consequence of the semiclassical description based on Eqs. (4) and (7), scaling properties of the underlying classical dynamics of the Rydberg electron should manifest themselves in the ionization spectra. On the classical level the trajectories $(\mathbf{x}(t),\mathbf{p}(t))$ and $(\tilde{\mathbf{x}}(t),\tilde{\mathbf{p}}(t))$ resulting from two spatially homogeneous HCPs with field strengths $\mathbf{E}(t)$ and $\tilde{\mathbf{E}}(t)=\gamma^4\mathbf{E}(\gamma^3t)$, $\gamma>0$, are related by the scaling transformation $\tilde{\mathbf{x}}(t)=\gamma^{-2}\mathbf{x}(\gamma^3t)$, $\tilde{\mathbf{p}}(t)=\gamma\mathbf{p}(\gamma^3t)$. In the impulse approximation this scaling relation has the far reaching consequence that the character of the classical dynamics depends on $\Delta\mathbf{p}^2$ and ϵ_0 only through the ratio $[\Delta\mathbf{p}^2/(-2\epsilon_0)]$, so that angle-resolved spectra for $(\epsilon_0,\Delta p,\epsilon^{(f)})$ and $(\gamma^2\epsilon_0,\gamma\Delta p,\gamma^2\epsilon^{(f)})$ will exhibit similar qualitative structure. As an example let us consider the case $\Delta\mathbf{p}^2/(-2\epsilon_0)=6.25$ in more detail. For the sake of comparison with fully quantum-mechanical results the corresponding examples are calculated for $n_0=50$, i.e., $\Delta p=0.05$ a.u., $l_0=0$, and $\alpha=0$. From Eq. (8) two characteristic dynamical regimes can be distinguished according to whether $\epsilon^{(f)}$ is smaller or larger than the critical energy $\epsilon_0+\Delta\mathbf{p}^2/2$ ($=28.6$ meV in this example). In both cases the dynamics of the ionization process are very different.

Classical trajectories with $0<\epsilon^{(f)}<\epsilon_0+\Delta\mathbf{p}^2/2$ start with negative (positive) radial momenta from the positive (negative) z half plane. Typical initial positions and final angles of trajectories, which according to Eq. (8) yield a particular

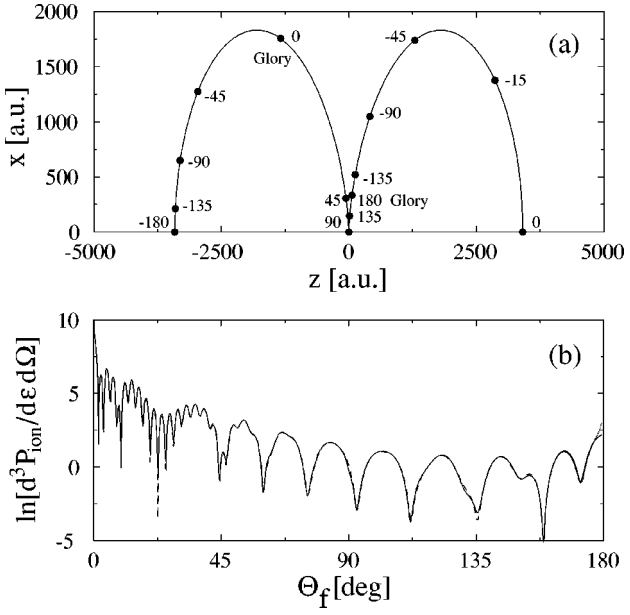

FIG. 1. (a) Full curve, initial positions of classical trajectories with $n_0=50$, $\Delta p=0.05$ a.u., and $\epsilon^{(f)}=10$ meV according to Eq. (8). The figure has to be continued into three dimensions by rotation around the z axis. The numbers indicate final emission angles for specific initial positions. The angle is counted counterclockwise from the z axis. (b) Angular distribution of the ionized electron $\ln\{d^3P_{ion}/(d\epsilon d\Omega)$[a.u.]$\}$ in the sudden ionization approximation for the parameter values given above: quantum-mechanical result (full), uniform semiclassical (dashed) and primitive semiclassical (dotted).

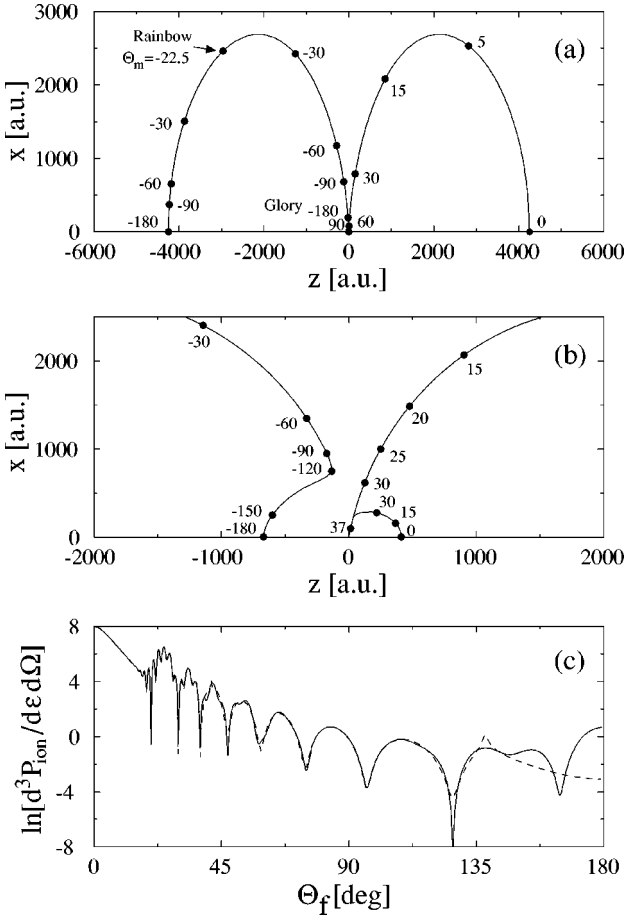

FIG. 2. (a) Same as Fig. 1(a) for $\epsilon^{(f)}=40$ meV. (b) Same as (a) for the pulse of finite duration described in the text. Shown is the region with the most significant modifications. Outside this region the figure would be similar to (a). (c) Angular distributions for the cases of (a) (full curve) and (b) (dashed).

final energy $\epsilon^{(f)}$, are depicted in Fig. 1(a) for a case with $\epsilon^{(f)}=10$ meV. Close inspection of Fig. 1(a) shows that for each final emission angle Θ_f there are three different corresponding initial positions. Therefore, one expects that the energy- and angle-resolved ionization probability exhibits a characteristic quantum-mechanical interference structure that originates from these three contributing trajectories. Furthermore, one notices that there are classical trajectories with $\Theta_f=0°(180°)$ whose initial positions do not lie on the z axis. The existence of these trajectories and the axial symmetry of the dynamics around the polarization axis of the HCP give rise to the semiclassical glory phenomenon [11]. It manifests itself in a divergence of the classical ionization density $(P^{(cl)})^2$ at $\Theta_f=0°$ and $\Theta_f=180°$, which originates from the coalescence of two axially symmetric families of classical trajectories. However, the resulting divergency of the primitive semiclassical result of Eq. (4) can be removed with the help of semiclassical uniformization methods [9,11].

In Fig. 1(b) the resulting energy- and angle-resolved ionization spectrum is depicted. In the sudden ionization approximation the result of a full quantum-mechanical calculation (full curve) is compared with the corresponding semiclassical uniform result (dashed curve) and the primitive semiclassical result based on Eq. (4) (dotted curve). The close agreement between the semiclassical and exact results is apparent. The quantum interference between the contributing classical trajectories leads to characteristic oscillations of the angular distribution. The angular distribution is concentrated around the glory angles $\Theta_f=0°,180°$ where the primitive semiclassical result diverges.

The characteristic behavior of classical trajectories with energies $1\gg\epsilon^{(f)}>\epsilon_0+\Delta\mathbf{p}^2/2$ is depicted in Fig. 2(a). In this case trajectories originating from the positive (negative) z half plane start with positive (negative) radial momenta. From Fig. 2(a) one notices an extremum of Θ_f on the curve of constant $\epsilon^{(f)}$. At the extremum final angle Θ_m the contributions of two classical trajectories coalesce and give rise to a semiclassical rainbow phenomenon and a divergence of the primitive semiclassical approximation. Again this divergence can be removed by uniformization methods [9,11]. In addition to this rainbow phenomenon, glory scattering appears at $\Theta_f=180°$. However, the glory phenomenon at $\Theta_f=0°$ that is present in the case of low electron energies has now disappeared. The full curve of Fig. 2(c) depicts the uniform semiclassical result for $d^3P_{ion}/[d\epsilon\wedge d\Omega]$ in the sudden ionization approximation. It is again almost indistinguishable from the corresponding quantum-mechanical calculation, which is not shown. For small Θ_f the spectrum is smooth as there is only one contributing trajectory. Around Θ_m, interference oscillations set in that reflect the appearance of two further trajectory classes. The three contributing trajectories persist up to $\Theta_f=180°$ where glory scattering is observed in the impulse approximation.

Finally, let us discuss the influence of realistic pulse forms on these ionization spectra with the help of Eqs. (4) and (7). Depending on the pulse duration and the spatial

pulse profile, various modifications of these angular distributions are expected to appear. They will be studied systematically in forthcoming work [9]. As an example, let us concentrate here on effects of finite pulse durations. Figure 2(b) depicts the modifications in the distribution of initial positions and final angles due to a moderately long HCP with pulse duration $\tau=0.01T_{cl}$ ($T_{cl}=2\pi n_0^3$ is the classical Kepler period of the Rydberg electron) and pulse form $\mathbf{E}(t)=\mathbf{e}_z E_0 \exp[-(t/\tau)^8]$. The amplitude E_0 is adjusted so that $|\Delta\mathbf{p}|=0.05$ a.u. as in the previous cases. It turns out that trajectories starting close to the nucleus are most sensitive to the pulse shape of an HCP. Three major modifications in the energy- and angle-resolved spectra can be recognized. (i) Trajectories with initially outgoing radial momenta lead to final angles with $|\Theta_f|<37.5°$, only. However, this hardly affects the spectrum [dashed curve in Fig. 2(c)], as the classical weight of this trajectory class decreases rapidly with increasing Θ_f already in the impulse approximation. (ii) A different class of trajectories with initially incoming radial momenta appears in the positive z half plane. They have final angles $|\Theta_f|<42°$ and give rise to small oscillations in the spectrum at small angles. (iii) The most profound changes are due to trajectories in the negative z half plane. Their initial positions change significantly so that the glory effect at $\Theta_f=180°$ disappears. Thus the spectrum is most sensitive to pulse-shape effects at large emission angles. The rainbow effect at small emission angles is rather insensitive to the pulse shape.

In summary, an alternative multidimensional semiclassical treatment of excitation of a Rydberg electron by an HCP has been presented. Based on this approach it has been shown that energy-resolved angular distributions of the ionized Rydberg electron exhibit characteristic oscillations that can be interpreted naturally as contributions of interfering classical trajectories. These quantum-mechanical interference features are dominated by semiclassical catastrophes of the glory and rainbow type. As all quantum-mechanical phases are taken into account properly, this semiclassical approach might also become a useful theoretical tool in problems concerning the reconstruction of quantum states of Rydberg electrons with the help of HCPs.

Support by the Deutsche Forschungsgemeinschaft, by the U.S. Office of Naval Research Contract No. 14-91-J1205, and by the U.S. Army Research Office is acknowledged. G.A. thanks H. P. Helm and P. U. Jepsen for stimulating discussions.

[1] R.R. Jones, D. You, and P.H. Bucksbaum, Phys. Rev. Lett. **70**, 1236 (1993); R.B. Vrijen, G.M. Lankhuijzen, and L.D. Noordam, *ibid.* **79**, 617 (1997).

[2] R.R. Jones, Phys. Rev. Lett. **76**, 3927 (1996).

[3] C. Raman *et al.*, Phys. Rev. Lett. **76**, 2436 (1996).

[4] C.O. Reinhold, H. Shaw, and J. Burgdörfer, J. Phys. B **27**, L469 (1994); K.J. La Gattuta and P.B. Lerner, Phys. Rev. A **49**, R1547 (1994); A. Bugacov *et al.*, *ibid.* **51**, 1490 (1995); M.T. Frey *et al.*, *ibid.* **55**, R865 (1997).

[5] M. Mallalieu and Shih-I Chu, Chem. Phys. Lett. **258**, 37 (1996).

[6] Ch. Bordas, Phys. Rev. A **58**, 400 (1998).

[7] H.A. Bethe and E. Salpeter, *Quantum Mechanics of One- and Two-electron Atoms* (Plenum, New York, 1977).

[8] V.P. Maslov and M.V. Fedoriuk, *Semiclassical Approximation in Quantum Mechanics* (Reidel, Boston, 1981).

[9] O. Zobay and G. Alber (unpublished).

[10] For a recent account of this work see, e.g., F. Grossmann, Comments At. Mol. Phys. (to be published), and references therein.

[11] M.V. Berry and K.E. Mount, Rep. Prog. Phys. **35**, 315 (1972).